JACS
JOURNAL OF THE AMERICAN CHEMICAL SOCIETY
Article
pubs.acs.org/JACS

Localized Excitation of Ti^{3+} Ions in the Photoabsorption and Photocatalytic Activity of Reduced Rutile TiO_2

Zhiqiang Wang,[†,#] Bo Wen,[‡,∥,#] Qunqing Hao,[†,#] Li-Min Liu,[*,‡] Chuanyao Zhou,[*,†] Xinchun Mao,[†] Xiufeng Lang,[‡] Wen-Jin Yin,[‡,⊥] Dongxu Dai,[†] Annabella Selloni,[*,§] and Xueming Yang[*,†]

[†]State Key Laboratory of Molecular Reaction Dynamics, Dalian Institute of Chemical Physics, Chinese Academy of Science, 457 Zhongshan Road, Dalian, 116023, Liaoning, P. R. China

[‡]Beijing Computational Science Research Center, Beijing, 100094, P. R. China

[§]Department of Chemistry, Princeton University, Princeton, New Jersey 08544, United States

[∥]International Center for Quantum Materials, Peking University, Beijing, 100871, P. R. China

[⊥]Chengdu Green Energy and Green Manufacturing Technology R&D Center, Chengdu, Sichuan 610207, P. R. China

Supporting Information

ABSTRACT: In reduced TiO_2, electronic transitions originating from the Ti^{3+}-induced states in the band gap are known to contribute to the photoabsorption, being in fact responsible for the material's blue color, but the excited states accessed by these transitions have not been characterized in detail. In this work we investigate the excited state electronic structure of the prototypical rutile TiO_2(110) surface using two-photon photoemission spectroscopy (2PPE) and density functional theory (DFT) calculations. Using 2PPE, an excited resonant state derived from Ti^{3+} species is identified at 2.5 ± 0.2 eV above the Fermi level (E_F) on both the reduced and hydroxylated surfaces. DFT calculations reveal that this excited state is closely related to the gap state at ∼1.0 eV below E_F, as they both result from the Jahn−Teller induced splitting of the 3*d* orbitals of Ti^{3+} ions in reduced TiO_2. Localized excitation of Ti^{3+} ions via 3*d* → 3*d* transitions from the gap state to this empty resonant state significantly increases the TiO_2 photoabsorption and extends the absorbance to the visible region, consistent with the observed enhancement of the visible light induced photocatalytic activity of TiO_2 through Ti^{3+} self-doping. Our work reveals the physical origin of the Ti^{3+} related photoabsorption and visible light photocatalytic activity in prototypical TiO_2 and also paves the way for the investigation of the electronic structure and photoabsorption of other metal oxides.

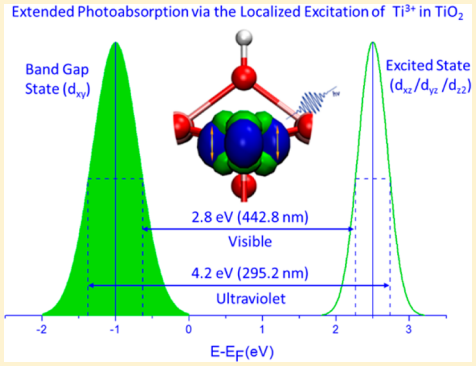

INTRODUCTION

Titanium dioxide (TiO_2) is well-known as one of the most widely used materials in photocatalysis and solar energy conversion.[1−9] All these applications are based on the generation of charge carriers by optical absorption, followed by their diffusion to the surface and transfer to adsorbed species. Stoichiometric rutile TiO_2 is an insulator with a band gap of ∼3 eV. In this material the photoexcitation involves transitions from the O 2p states in the valence band (VB) to the 3d states of the Ti (formally Ti^{4+}) cations in the conduction band (CB). TiO_2 is very easily reduced, however. The reduction is accompanied by the formation of Ti^{3+} ions, for which a characteristic signature is the presence of a localized state in the band gap at ∼0.8−1 eV below the CB edge. Many studies have focused on the Ti^{3+}-induced gap states and their possible role in TiO_2 photocatalysis in recent years.[10−13] There is evidence that *d* → *d* transitions from the gap states contribute to the photoabsorption of reduced TiO_2, as indicated by the material's blue color,[14] whose intensity increases with the degree of reduction. Because of the band gap narrowing and enhanced photoabsorption associated with the presence of the Ti^{3+} induced band gap state, visible light photocatalysis through Ti^{3+} self-doping has also been achieved.[15−19] While transitions from the band gap state are clearly important, little is known, however, about the character of the electronic excited states that are involved in these transitions, due also to the greater difficulty to experimentally access unoccupied states in comparison to occupied ones. A characterization of these states is not only scientifically interesting but also important for a better understanding and control of TiO_2 photocatalysis.

In this work we utilize two-photon photoemission spectroscopy (2PPE) measurements in combination with density functional theory (DFT) calculations to investigate the excited states of the rutile TiO_2(110) surface, a well-established model system for surface science[3,5,20−22] and theoretical[23−27] studies of TiO_2. 2PPE, which employs a 1 + 1 pump−probe scheme, is an ideal technique to investigate excited states. In the two-photon excitation process (shown schematically in Figure S1), population of an intermediate state is followed by emission to a

Received: May 7, 2015
Published: June 29, 2015

DOI: 10.1021/jacs.5b04483
J. Am. Chem. Soc. 2015, 137, 9146−9152

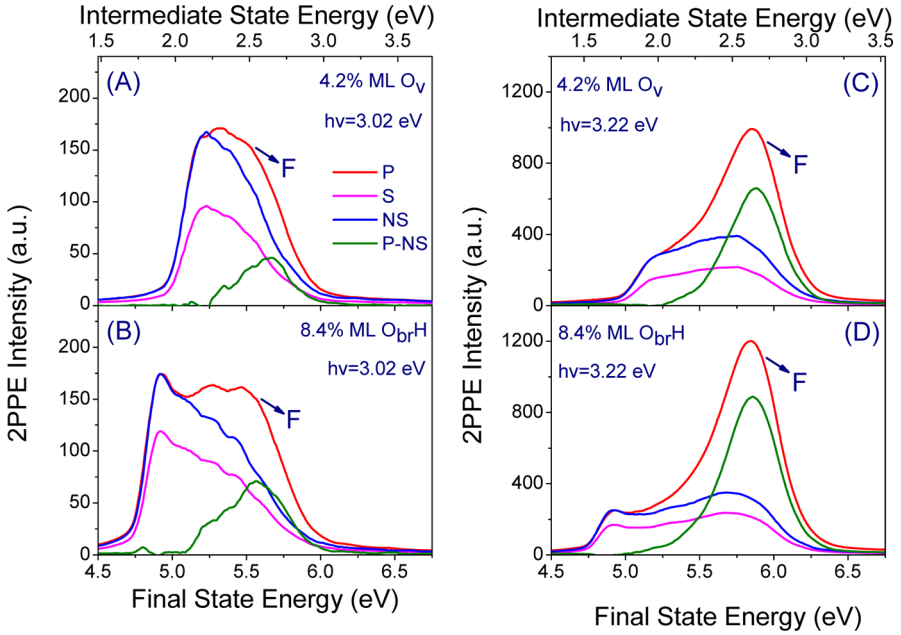

Figure 1. Typical 2PPE spectra for the *r*-TiO_2(110) (A and C) and *h*-TiO_2(110) (B and D) surfaces. The spectra were measured with both *p*-polarized (P) and *s*-polarized (S) light with a photon energy of 3.02 eV (A and B) and 3.22 eV (C and D) respectively. For comparison, S was normalized to P at the secondary electron signal edge. P-NS denotes the difference spectra, which was obtained by subtracting the normalized *s*-polarized data (NS) from the *p*-polarized data. The curves were smoothed by averaging the adjacent seven data points. The signal was integrated from −5 degrees to +5 degrees. Energies are measured with respect to E_F; those in the top *X*-axis refer to the intermediate state, before absorption of the second photon. Note the different intensity scales of the spectra on the left (A and B) and right (C and D) panels.

final state above the vacuum level through absorption of a second photon. By 2PPE we observe an excited state centered at 2.5 ± 0.2 eV above the Fermi energy (E_F; hereafter, all energies are measured with respect to E_F) on both the clean reduced and hydroxylated TiO_2(110) surfaces, indicating that this is an intrinsic state associated with the Ti^{3+} species in the reduced samples. DFT calculations further reveal that, similarly to the gap state at ∼0.8−1.0 eV below E_F, the excited resonant state originates from the Jahn−Teller induced splitting of the 3*d* orbitals of Ti^{3+} ions. This state can be accessed via $d \rightarrow d$ transitions from the gap state and increases significantly the photoabsorption of reduced TiO_2. Owing to the relative wide distribution of both the band gap state and excited state, the absorbance from $d \rightarrow d$ transitions ranges from the UV to the visible region, in agreement with the observed enhancement of the TiO_2 photocatalytic activity under visible light irradiation through Ti^{3+} self-doping.[15−19,28] The present work not only provides a better understanding of the Ti^{3+} related visible light photocatalytic activity of the prototypical TiO_2 but also paves the way for the investigation of the electronic structure and photoabsorption of other metal oxides.

EXPERIMENTAL AND THEORETICAL DETAILS

All experiments were performed in a ultrahigh vacuum (UHV) apparatus (base pressure better than 5×10^{-11} mbar), which has been described in detail previously.[29] TiO_2(110) samples (Princeton Scientific Corp.) were prepared by cycles of Ar^+ sputtering and UHV annealing at 850 K, generating a reduced substrate (*r*-TiO_2(110)). The cleanness and long-range order were confirmed by Auger electron spectroscopy (AES) and low energy electron diffraction (LEED), respectively. The concentration of the bridging oxygen vacancy (O_v) was determined to be 4.2% monolayer (ML; 1ML = 5.2×10^{14} cm^{-2}) by temperature-programmed desorption (TPD) of water.[30] Hydroxylated TiO_2(110) (*h*-TiO_2(110)) was prepared by photocatalyzed splitting of methanol on this surface,[31] which was then heated to 370 K to remove species adsorbed on fivefold coordinated Ti (Ti_{5c}) sites. Methanol dissociates spontaneously at O_v sites, producing bridging methoxy (CH_3O_{br}) and hydroxyl ($O_{br}H$) groups.[32] To minimize the amount of CH_3O_{br}, *r*-TiO_2(110) was first exposed to excess water followed by heating to 350 K to convert all the O_v to $O_{br}H$.[33] The residual water on Ti_{5c} sites after this procedure is below the detection limit of the mass spectrometer. Purified methanol was then dosed onto this surface and exposed to ultraviolet (UV) light. It should be pointed out that with this procedure 3.0% ML CH_3O_{br} still remains due to displacement,[34] but the same amount of CH_3O_{br} and $O_{br}H$ contribute equally to the excited resonance signal (Figure S2). The second harmonic (SH, 2.95−3.59 eV) of a Ti: Sapphire oscillator (Spectra-Physics, MaiTai eHP DeepSee) was delivered in pulses of 90 fs duration and 1.5 nJ at an 80-MHz repetition rate. All photoemission measurements were performed with a TiO_2 sample temperature of 120 K.

DFT calculations were performed with the CP2K/Quickstep package,[35] which uses a hybrid Gaussian and plane-waves approach. The hybrid HSE06 functional[36−38] was chosen for all the calculations. For comparison with the HSE06 results, selected calculations using the B3LYP hybrid functional[39] were also performed. Core electrons were described with norm-conserving Goedecker, Teter, and Hutter (GTH) pseudopotentials.[40] The wave functions of the valence electrons were expanded in terms of Gaussian functions with molecularly optimized double-ζ polarized basis sets (m-DZVP), which ensures a small basis set superposition error.[41] For the auxiliary basis set of plane waves a 280 Ry cutoff was used. Reciprocal space sampling was restricted to the Γ point.

The rutile-TiO_2(110) surface was modeled using a repeated slab geometry with slabs of four TiO_2 trilayers and a (4 × 2) (11.836 Å × 12.994 Å) surface cell. The vacuum separation between slabs was around 15 Å. Hydroxylated TiO_2(110) surfaces were modeled by adding 1, 2, and 4 hydrogen atoms to the surface bridging oxygen sites, corresponding to $O_{br}H$ coverages of 1/8 ML, 1/4 ML, and 1/2 ML, respectively. Reduced surfaces were modeled by removing one bridging oxygen atom per unit cell. All atoms in the slab were relaxed until the maximum residual force is less than 0.02 eV/Å. We note that

DOI: 10.1021/jacs.5b04483
J. Am. Chem. Soc. 2015, 137, 9146−9152

the theoretical hydroxyl/defect concentration is generally larger than the experimental one. As shown below, however, the properties of the excited state do not depend on the defect concentration except for the intensity. Therefore, it is well justified to connect the experimental and theoretical results in the present study.

RESULTS AND DISCUSSION

Polarization dependent 2PPE spectra for different $TiO_2(110)$ surfaces and excitation energies are compared in Figure 1. Since in our samples E_F is close to the CB edge and the work function is 4.8−5.1 eV, electrons in the VB cannot be excited into vacuum via two-photon photoemission with the photon energy used in our work. Therefore, the only possible initial states of the observed photoelectrons are the Ti^{3+} induced states in the band gap. Figure 1A shows the 2PPE spectrum for the clean reduced surface, *r*-$TiO_2(110)$, acquired at an excitation energy of 3.02 eV, a value similar to that used in previous studies on water or alcohol covered $TiO_2(110)$.[42−45] A small additional feature (labeled as F) around 2.5 eV above E_F is observed in the *p*-polarized 2PPE (*p*-2PPE) spectrum relative to *s*-polarized 2PPE. When the O_v's on *r*-$TiO_2(110)$ are titrated by water, bridging hydroxyls ($O_{br}H$'s) are produced, resulting in a hydroxylated surface.[33] The 2PPE spectra for *r*-$TiO_2(110)$ (Figure 1A) and *h*-$TiO_2(110)$ (Figure 1B) are clearly similar, suggesting that O_v and $O_{br}H$ contribute similarly to the unoccupied states of $TiO_2(110)$, as found also for the occupied state in the band gap.[11,46,47]

The feature F in Figure 1A and 1B is similar but much smaller than the one observed at 2.3−2.4 eV above E_F on water or alcohol covered $TiO_2(110)$.[42−45] This is the reason why this feature was ignored for bare TiO_2 in previous studies. Instead, the strong resonance on water or alcohol covered $TiO_2(110)$ was ascribed to a "wet electron" state (induced by the simultaneous presence of bridging hydroxyls and a water monolayer on water/$TiO_2(110)$[42] and methyl groups of methanol/methoxy and bridging hydroxyl groups on methanol/$TiO_2(110)$,[43] respectively) or to the dissociation of alcohols on the $TiO_2(110)$ surface.[44,48] An important reason why the excited resonance signal is more prominent on water or alcohol covered $TiO_2(110)$ than on the bare surface is however that water or alcohol adsorption significantly reduces the work function,[49,50] leading to the separation of the secondary electrons and the excited resonance signal in 2PPE spectra. An alternative way to increase the signal separation without adding adsorbates is to raise the 2PPE excitation photon energy. This increases the kinetic energy of the photoelectrons of interest, thus allowing their separation from the secondary electrons, and also excites electrons closer to the maxima of the band gap states which are the initial states in the present 2PPE measurements. As shown in Figure 1C and 1D, feature F in the 2PPE spectra of *r*-$TiO_2(110)$ and *h*-$TiO_2(110)$ becomes indeed much more pronounced with an excitation photon energy of 3.22 eV, thus confirming that this resonance is not due to adsorbates but is rather an ***intrinsic*** property of the $TiO_2(110)$ surface.

2PPE spectra include information on both initial and intermediate states. In order to determine the origin of the resonant feature F, both one-photon photoemission (1PPE) and 2PPE spectra with similar initial and final states were measured on an *h*-$TiO_2(110)$ with 3.0% ML CH_3O_{br} and 15.4% ML $O_{br}H$. Since equal amounts of CH_3O_{br} and $O_{br}H$ contribute equivalently to the resonant feature F (Figure S2), CH_3O_{br} was regarded as $O_{br}H$ in the present experiments. An excitation energy of 5.9 eV was used for the 1PPE, and correspondingly a photon energy of 2.95 eV, half of that for the 1PPE, was used for the 2PPE measurements (see Figure S1). From the normalized photoemission spectra in Figure 2A, it

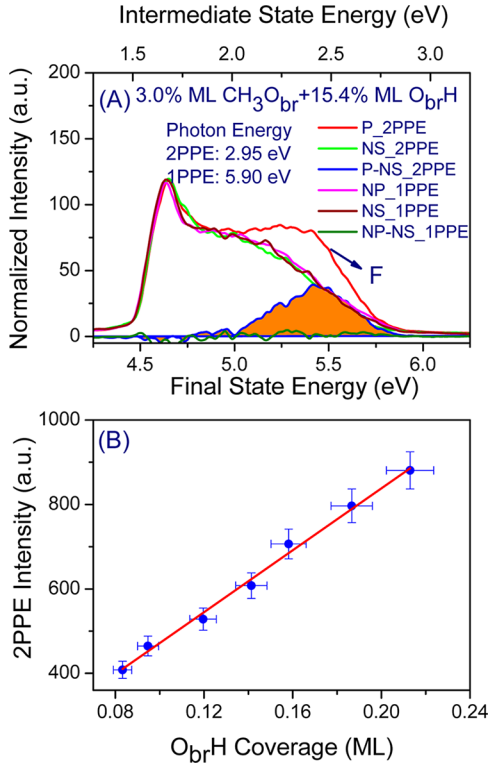

Figure 2. (A) 1PPE and 2PPE spectra of an *h*-$TiO_2(110)$ surface with 3.0% ML CH_3O_{br} and 15.4% ML $O_{br}H$. The excitation photon energies for 1PPE and 2PPE were 5.90 and 2.95 eV, respectively. The signal in these spectra was integrated from −5 degrees to +5 degrees. Energies are measured with respect to the Fermi level. Except *p*-2PPE, the normalized *s*-2PPE, *p*-1PPE, and *s*-1PPE spectra are identical, suggesting feature F detected by *p*-2PPE is from an intermediate state. (B) $O_{br}H$ coverage dependence of the excited resonance signal.

appears that *s*-2PPE, *p*-1PPE, and *s*-1PPE from an *h*-$TiO_2(110)$ surface are nearly identical, and do not show any feature at ∼2.5 eV above E_F. At variance with the other spectra, *p*-2PPE clearly displays feature F. This feature is present in 2PPE and absent in 1PPE, indicating that it originates from the intermediate state. The lifetime of the excited state was then examined by time-resolved two-photon photoemission (TR-2PPE) with a 3.14 eV and 28 fs pulse (SHG from an oscillator, Femtolasers Produktions GmbH). The two-pulse correlation from the excited state overlaps completely with the autocorrelation from a polycrystalline molybdenum surface, suggesting the lifetime of the excited state is too short to measure, as found also in a previous study.[42] Nonetheless, by comparing the two-pulse correlation from the clean reduced $TiO_2(110)$ and those covered by water or methanol,[42,43,48] an upper limit of 20 fs for the lifetime of the intrinsic excited state could be estimated, in accord with its spectral width of 0.5−0.6 eV.

To characterize the nature of the excited state, $TiO_2(110)$ surfaces with different amounts of point defects (for example, surface $O_{br}H$, surface O_v, and subsurface Ti interstitials) are desirable. However, due to the difficulty to quantitatively assess the concentration of subsurface Ti interstitials accompanying the creation of surface O_v's by conventional sputtering and

DOI: 10.1021/jacs.5b04483
J. Am. Chem. Soc. 2015, 137, 9146−9152

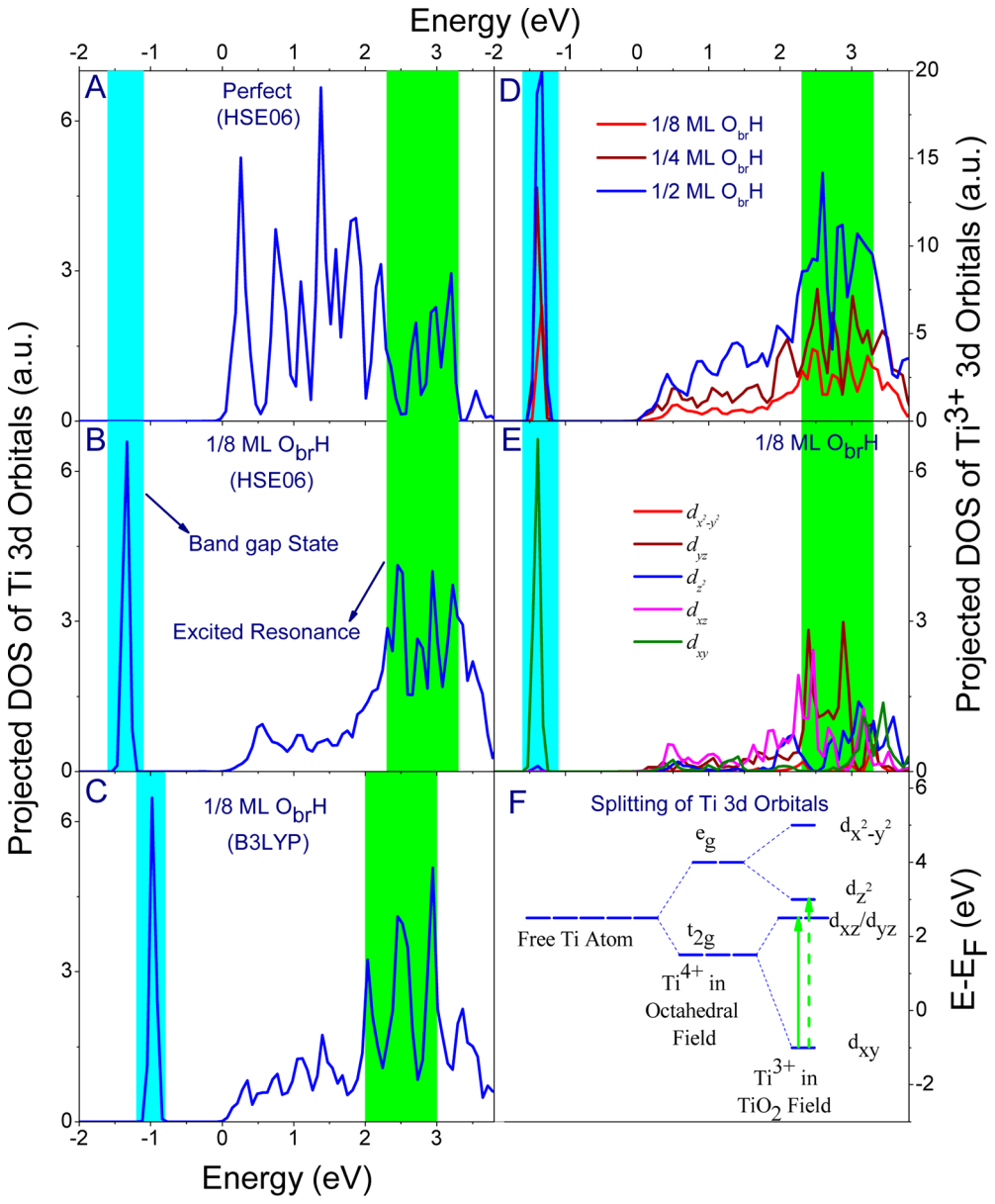

Figure 3. Projected density of states for Ti 3*d* orbitals: (A) Ti^{4+} ion in defect-free TiO_2(110), calculated using the HSE06 functional; (B) Ti^{3+} ion on *h*-TiO_2(110) with 1/8 ML $O_{br}H$, calculated using the HSE06 functional; (C) same as (B), but calculated using the B3LYP functional. (D) Total projected DOS of Ti^{3+} 3*d* orbitals in TiO_2(110) with 1/8 ML (red), 1/4 ML (wine), and 1/2 ML (blue) hydroxyls ($O_{br}H$). (E) Contributions of various *d* suborbitals to the projected DOS of Ti^{3+} 3*d* orbitals in TiO_2(110) with 1/8 ML $O_{br}H$. The cyan and light green bars highlight the computed band gap state and excited resonance, respectively. (F) Crystal field splitting of Ti 3*d* orbitals on TiO_2(110). The positions of the energy levels have been drawn at approximately the centers of gravity of the corresponding projected DOS (see Figure S4). The experimentally observed excited resonance at 2.5 ± 0.2 eV originates from the transitions indicated by the full vertical green line, with a smaller contribution from the transitions indicated by the dashed line as well. The energy zero is at the Fermi energy (E_F) which is taken coincident with the bottom of the conduction band.

annealing,[51] we rather vary the density of surface bridging hydroxyls through photocatalyzed splitting of methanol[13,31] which is a much milder method to introduce point defects (see details in the Experimental and Theoretical Details section). Figure 2B shows 2PPE spectra of *h*-TiO_2(110) as a function of $O_{br}H$ coverage. Feature F increases with the $O_{br}H$ density, leading to a linear relation between the integrated signal from the excited resonance and the $O_{br}H$ density. Since both oxygen vacancies and bridging hydroxyls are directly related to the reduction of the TiO_2 surface, this linear relationship suggests that the excited state is associated with Ti^{3+} species. Such a conclusion is also supported by previous inverse photoemission spectroscopy (IPS) studies, which have shown that the density of states (DOS) around 3 eV above E_F increases dramatically with the exposure of TiO_2(110) to Ar ions.[52,53] Since Ar ion sputtering preferentially removes oxygen, the changes of DOS above E_F in the IPS spectra are related to the reduction of Ti ions, consistent with our results.

We further explored the character of the intermediate state observed in 2PPE by DFT hybrid functional calculations, focusing on the Ti-derived states near E_F (here assumed to be at the CB minimum). Figure 3A and 3B show Ti-projected densities of states (PDOSs) for defect-free and 1/8 ML $O_{br}H$-covered TiO_2(110) obtained using the HSE06 functional,[37]

DOI: 10.1021/jacs.5b04483
J. Am. Chem. Soc. 2015, 137, 9146−9152

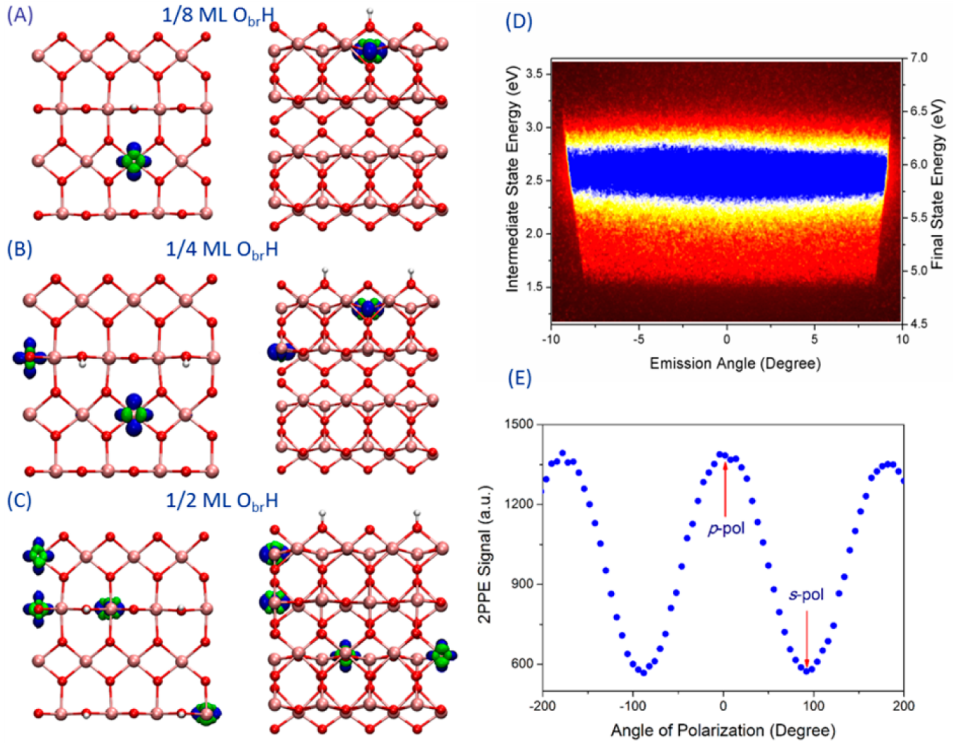

Figure 4. (A–C) Spin densities of the gap states (blue contours) and the excited resonant states at 2.5 ± 0.2 eV (green contours) on *h*-TiO_2(110) with different coverages of bridging hydroxyls: 1/8 (A), 1/4 (B) and 1/2 ML (C), respectively. The pink, red, and white spheres represent titanium, oxygen, and hydrogen atoms, respectively. Left panel: top-view, along [110]; right panel: side-view, along [1$\bar{1}$0]. (D) Angle-resolved *p*-2PPE spectra for the *h*-TiO_2(110) surface with 8.4% ML $O_{br}H$. The excitation photon energy is 3.35 eV. There is little angular dispersion of the excited state, suggesting the state is localized. (E) Polarization dependence of the 2PPE excited resonance signal.

which is known to provide an accurate description of the electronic structure of a wide range of materials. In the PDOS of Ti^{4+} cations on the stoichiometric surface (Figure 3A) we can notice two groups of electronic states, corresponding to the Ti *3d* t_{2g}- and e_g-like states found in bulk TiO_2[54,55] (see also below). A very different shape is observed instead for the PDOS of a Ti^{3+} center on the hydroxylated surface (Figure 3B). Besides the gap state at ∼1 eV below E_F, extensively discussed in previous studies,[13,46,56] the latter shows a reduced number of states in the range 0–2 eV and a clear enhancement above ∼2.3 eV in comparison to the PDOS of a Ti^{4+} ion. Except for some small differences in the energy positions, these general features of the PDOS of Ti^{3+} ions are confirmed by calculations performed using B3LYP,[39] a hybrid functional employed in several previous studies of defects in TiO_2[46] (Figure 3C). This indicates that the presence of Ti^{3+} derived resonant states in the range ∼2–3 eV is a robust feature of the electronic structure of *h*-TiO_2(110) that does not depend on the hybrid functional used for the calculations. Furthermore, computed PDOS curves for Ti^{3+} ions on reduced TiO_2(110) surfaces with oxygen vacancies and Ti interstitials are qualitatively similar to those found for Ti^{3+} on *h*-TiO_2(110) (Figure S3), in agreement with the 2PPE observation that this resonance is an inherent characteristics of Ti^{3+} species that does not depend on the presence of adsorbates. As the coverage of $O_{br}H$ increases, both the band gap state and the excited resonance become more intense (Figure 3D), which is also in accord with the 2PPE results.

It is interesting to consider the contribution of the different *d* orbitals to the PDOS of Ti^{3+} ions (Figures 3E, S4, and S5). In bulk TiO_2, the Ti ions occupy slightly distorted octahedral sites; thus, their 3*d* orbitals split into two distinct groups, a lower group of three orbitals (d_{xy}, d_{yz} and d_{xz}) with t_{2g}-like symmetry and an upper group of two orbitals ($d_{x^2-y^2}$ and d_{z^2}) with e_g-like symmetry.[54] In stoichiometric TiO_2, the t_{2g}-like orbitals contribute mainly to the conduction band minimum. On hydroxylated or reduced TiO_2(110), the t_{2g}^1 configuration of Ti^{3+} ions leads to a Jahn–Teller distortion, which further splits the three t_{2g} orbitals into a low energy state with d_{xy} character and two high energy orbitals with d_{yz} and d_{xz} character (Figure 3F). Excess electrons from reducing defects fill the d_{xy} orbitals giving rise to the occupied polaronic state in the band gap,[46] while the d_{yz} and d_{xz} orbitals move to higher energy and give rise to the excited resonance at ∼2–3 eV above E_F. Plots of the gap and excited states on hydroxylated TiO_2(110) surfaces with different $O_{br}H$ coverages are reported in Figure 4A–C (here the states in the energy window 2.5 ± 0.2 eV were selected). The excited state appears to maintain a *d*-like character and remain fairly localized despite being resonant with the TiO_2 CB. The latter result is well supported by our angle-resolved 2PPE measurements (Figure 4D).

Based on the above analysis, the feature F observed in 2PPE should be attributed to localized excitation of Ti^{3+} ions via $d \rightarrow d$ transitions from the gap state to the unoccupied excited state. On TiO_2(110) the three main symmetry directions are [110], [1$\bar{1}$0], and [001]. The latter corresponds to the direction of the strands of edge-sharing (slightly distorted) TiO_6 octahedra in the rutile structure, while [110] and [1$\bar{1}$0] correspond to the directions of the main axes of the TiO_6 octahedra along the strands. This suggests that the intra-atomic Ti^{3+} $d \rightarrow d$ transitions should be easily excited by polarized light with the electric field parallel to [110] or [1$\bar{1}$0], whereas these

DOI: 10.1021/jacs.5b04483
J. Am. Chem. Soc. 2015, 137, 9146–9152

transitions should be forbidden or much weaker when the field is parallel to [001]. Our polarization dependent 2PPE results agree well with this prediction. In our measurements, the [1$\bar{1}$0] direction is in the incidence plane; thus, the components of the electric field of *p*-polarized light are along [110] and [1$\bar{1}$0], while those of *s*-polarized light are along [001] (Figure S6). From Figure 4E one can see that as the polarization is varied gradually from *s* to *p*, the signal of peak F increases monotonically. In fact, the signal changes periodically with the polarization, with maxima and minima at *p*- and *s*-polarization, respectively. Since the profiles of *s*-2PPE and 1PPE are nearly identical (Figure 2A), the signal in *s*-2PPE comes from the band gap states at ∼0.8−1.0 eV below E_F without populating the excited state at ∼2.5 eV above E_F; in other words, *s*-polarized light is "blind" to the excited state. Only by using polarized light with the electric field along [110] and/or [1$\bar{1}$0] can we detect the excited state, consistent with our symmetry analysis.

SUMMARY

In summary, in this work we have identified an excited resonant state centered at 2.5 ± 0.2 eV above E_F associated with Ti^{3+} species in reduced TiO_2. By DFT calculations, we have shown that this excited state is closely related to the band gap state, as they both result from the Jahn−Teller-induced splitting of the 3*d* orbitals of Ti^{3+} ions. The $d \rightarrow d$ transitions from the Ti^{3+} related occupied band gap state at ∼−(0.8−1.0) eV to the empty excited state at ∼2.5 eV increase the photoabsorption in the ultraviolet (UV) region. At the same time, the relative wide distribution of these two states also extends the absorbance to the visible range (Figure 5). This extended photoabsorption together with the near-infrared absorption produce an absorption minimum in the blue, which is the reason why reduced TiO_2 samples appear as blue.[14] In addition, the $d \rightarrow d$ transitions that we have identified explain the underlying mechanism of the enhanced and extended absorption of reduced TiO_2 in the visible region, leading to a better understanding of the enhanced visible light photocatalytic activity through Ti^{3+} self-doping.[15−19,28] Our work also paves the way for the investigation of the electronic structure and photoabsorption of other metal oxides.

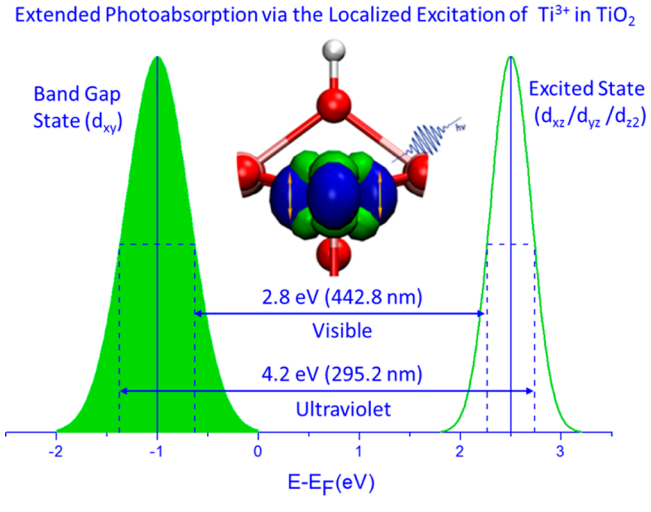

Figure 5. Schematic of the enhanced and extended photoabsorption via $3d \rightarrow 3d$ transitions from the band gap state to the excited resonant state at 2.5 ± 0.2 eV in reduced TiO_2 (see Figure 3F for details). Blue and green charge density isosurfaces in the middle panel represent the band gap and excited states, respectively. The experimentally measured fwhm (full width at half maxima) of the band gap state and the excited state are ∼0.8 eV[12,47] and ∼0.5 eV, respectively.

ASSOCIATED CONTENT

Supporting Information

Schematic of one-photon photoemission (1PPE) and two-photon photoemission (2PPE) from TiO_2. Contribution of $O_{br}H$ and CH_3O_{br} to the excited state. Projected DOS of Ti^{3+} 3*d* orbitals in TiO_2(110) slabs containing Ti interstitials or oxygen vacancies calculated with the HSE06 functional. Contributions of different *d* orbitals to the projected DOS of Ti^{3+} 3*d* states in 1/8 ML $O_{br}H$ covered TiO_2(110) and Ti^{4+} 3*d* states in stoichiometric TiO_2(110). Contributions of different *d* orbitals to the projected DOS of Ti^{3+} 3*d* states on TiO_2(110) covered with 1/4 ML and 1/2 ML bridging hydroxyls. Schematic overview of the experimental geometry. The Supporting Information is available free of charge on the ACS Publications website at DOI: 10.1021/jacs.5b04483.

AUTHOR INFORMATION

Corresponding Authors

*limin.liu@csrc.ac.cn
*chuanyaozhou@dicp.ac.cn
*aselloni@princeton.edu
*xmyang@dicp.ac.cn

Author Contributions

#Z.W., B.W., and Q.H. contributed equally.

Notes

The authors declare no competing financial interest.

ACKNOWLEDGMENTS

We thank Ulrike Diebold and Andrea Vittadini for a critical reading of our manuscript. C.Z., L.L., and X.Y. acknowledge the financial support from the National Natural Science Foundation of China (Grant Nos. 21203189, 21321091, 51222212), the Ministry of Science and Technology of China (Grant Nos. 2013CB834605, 2011CB922200), the Key Research Program of the Chinese Academy of Science (Grant No. KGZD-EW-T05), and the State Key Laboratory of Molecular Reaction Dynamics (Grant No. ZZ-2014-02). A.S. acknowledges the support of DoE-BES, Division of Chemical Sciences, Geosciences and Biosciences under Award DE-FG02-12ER16286.

REFERENCES

(1) Linsebigler, A. L.; Lu, G. Q.; Yates, J. T. *Chem. Rev.* **1995**, *95*, 735.
(2) Gratzel, M. *Nature* **2001**, *414*, 338.
(3) Diebold, U. *Surf. Sci. Rep.* **2003**, *48*, 53.
(4) Fujishima, A.; Zhang, X.; Tryk, D. A. *Surf. Sci. Rep.* **2008**, *63*, 515.
(5) Henderson, M. A. *Surf. Sci. Rep.* **2011**, *66*, 185.
(6) Schneider, J.; Matsuoka, M.; Takeuchi, M.; Zhang, J.; Horiuchi, Y.; Anpo, M.; Bahnemann, D. W. *Chem. Rev.* **2014**, *114*, 9919.
(7) Ma, Y.; Wang, X.; Jia, Y.; Chen, X.; Han, H.; Li, C. *Chem. Rev.* **2014**, *114*, 9987.
(8) Bai, Y.; Mora-Seró, I.; De Angelis, F.; Bisquert, J.; Wang, P. *Chem. Rev.* **2014**, *114*, 10095.
(9) Thompson, T. L.; Yates, J. T. *Chem. Rev.* **2006**, *106*, 4428.
(10) Henrich, V. E.; Dresselhaus, G.; Zeiger, H. J. *Phys. Rev. Lett.* **1976**, *36*, 1335.
(11) Yim, C. M.; Pang, C. L.; Thornton, G. *Phys. Rev. Lett.* **2010**, *104*, 036806.

DOI: 10.1021/jacs.5b04483
J. Am. Chem. Soc. 2015, 137, 9146−9152

(12) Wendt, S.; Sprunger, P. T.; Lira, E.; Madsen, G. K. H.; Li, Z. S.; Hansen, J. O.; Matthiesen, J.; Blekinge-Rasmussen, A.; Laegsgaard, E.; Hammer, B.; Besenbacher, F. *Science* **2008**, *320*, 1755.
(13) Mao, X. C.; Lang, X. F.; Wang, Z. Q.; Hao, Q. Q.; Wen, B.; Ren, Z. F.; Dai, D. X.; Zhou, C. Y.; Liu, L. M.; Yang, X. M. *J. Phys. Chem. Lett.* **2013**, *4*, 3839.
(14) Khomenko, V. M.; Langer, K.; Rager, H.; Fett, A. *Phys. Chem. Miner.* **1998**, *25*, 338.
(15) Justicia, I.; Ordejon, P.; Canto, G.; Mozos, J. L.; Fraxedas, J.; Battiston, G. A.; Gerbasi, R.; Figueras, A. *Adv. Mater.* **2002**, *14*, 1399.
(16) Zuo, F.; Wang, L.; Wu, T.; Zhang, Z. Y.; Borchardt, D.; Feng, P. Y. *J. Am. Chem. Soc.* **2010**, *132*, 11856.
(17) Zuo, F.; Bozhilov, K.; Dillon, R. J.; Wang, L.; Smith, P.; Zhao, X.; Bardeen, C.; Feng, P. *Angew. Chem., Int. Ed.* **2012**, *51*, 6223.
(18) Mao, C. Y.; Zuo, F.; Hou, Y.; Bu, X. H.; Feng, P. Y. *Angew. Chem., Int. Ed.* **2014**, *53*, 10485.
(19) Zuo, F.; Wang, L.; Feng, P. Y. *Int. J. Hydrogen Energy* **2014**, *39*, 711.
(20) Dohnalek, Z.; Lyubinetsky, I.; Rousseau, R. *Prog. Surf. Sci.* **2010**, *85*, 161.
(21) Henderson, M. A.; Lyubinetsky, I. *Chem. Rev.* **2013**, *113*, 4428.
(22) Pang, C. L.; Lindsay, R.; Thornton, G. *Chem. Rev.* **2013**, *113*, 3887.
(23) Rossmeisl, J.; Qu, Z. W.; Zhu, H.; Kroes, G. J.; Norskov, J. K. *J. Electroanal. Chem.* **2007**, *607*, 83.
(24) Kowalski, P. M.; Camellone, M. F.; Nair, N. N.; Meyer, B.; Marx, D. *Phys. Rev. Lett.* **2010**, *105*, 146405.
(25) Deskins, N. A.; Rousseau, R.; Dupuis, M. *J. Phys. Chem. C* **2011**, *115*, 7562.
(26) Cheng, J.; Liu, X.; Kattirtzi, J. A.; VandeVondele, J.; Sprik, M. *Angew. Chem., Int. Ed.* **2014**, *53*, 12046.
(27) Cheng, J.; VandeVondele, J.; Sprik, M. *J. Phys. Chem. C* **2014**, *118*, 5437.
(28) Zhou, C.; Ma, Z.; Ren, Z.; Mao, X.; Dai, D.; Yang, X. *Chemical Science* **2011**, *2*, 1980.
(29) Ren, Z. F.; Zhou, C. Y.; Ma, Z. B.; Xiao, C. L.; Mao, X. C.; Dai, D. X.; LaRue, J.; Cooper, R.; Wodtke, A. M.; Yang, X. M. *Chin. J. Chem. Phys.* **2010**, *23*, 255.
(30) Henderson, M. A. *Surf. Sci. Rep.* **2002**, *46*, 1.
(31) Guo, Q.; Xu, C.; Ren, Z.; Yang, W.; Ma, Z.; Dai, D.; Fan, H.; Minton, T. K.; Yang, X. *J. Am. Chem. Soc.* **2012**, *134*, 13366.
(32) Zhang, Z. R.; Bondarchuk, O.; White, J. M.; Kay, B. D.; Dohnalek, Z. *J. Am. Chem. Soc.* **2006**, *128*, 4198.
(33) Bikondoa, O.; Pang, C. L.; Ithnin, R.; Muryn, C. A.; Onishi, H.; Thornton, G. *Nat. Mater.* **2006**, *5*, 189.
(34) Henderson, M. A.; Otero-Tapia, S.; Castro, M. E. *Faraday Discuss.* **1999**, *114*, 313.
(35) VandeVondele, J.; Krack, M.; Mohamed, F.; Parrinello, M.; Chassaing, T.; Hutter, J. *Comput. Phys. Commun.* **2005**, *167*, 103.
(36) Heyd, J.; Scuseria, G. E.; Ernzerhof, M. *J. Chem. Phys.* **2003**, *118*, 8207.
(37) Krukau, A. V.; Vydrov, O. A.; Izmaylov, A. F.; Scuseria, G. E. *J. Chem. Phys.* **2006**, *125*, 224106.
(38) Guidon, M.; Hutter, J.; VandeVondele, J. *J. Chem. Theory Comput.* **2009**, *5*, 3010.
(39) Becke, A. D. *J. Chem. Phys.* **1993**, *98*, 1372.
(40) Goedecker, S.; Teter, M.; Hutter, J. *Phys. Rev. B: Condens. Matter Mater. Phys.* **1996**, *54*, 1703.
(41) VandeVondele, J.; Hutter, J. *J. Chem. Phys.* **2007**, *127*, 114105.
(42) Onda, K.; Li, B.; Zhao, J.; Jordan, K. D.; Yang, J. L.; Petek, H. *Science* **2005**, *308*, 1154.
(43) Li, B.; Zhao, J.; Onda, K.; Jordan, K. D.; Yang, J. L.; Petek, H. *Science* **2006**, *311*, 1436.
(44) Zhou, C. Y.; Ren, Z. F.; Tan, S. J.; Ma, Z. B.; Mao, X. C.; Dai, D. X.; Fan, H. J.; Yang, X. M.; LaRue, J.; Cooper, R.; Wodtke, A. M.; Wang, Z.; Li, Z. Y.; Wang, B.; Yang, J. L.; Hou, J. G. *Chemical Science* **2010**, *1*, 575.
(45) Ma, Z.; Guo, Q.; Mao, X.; Ren, Z.; Wang, X.; Xu, C.; Yang, W.; Dai, D.; Zhou, C.; Fan, H.; Yang, X. *J. Phys. Chem. C* **2013**, *117*, 10336.
(46) Di Valentin, C.; Pacchioni, G.; Selloni, A. *Phys. Rev. Lett.* **2006**, *97*, 166803.
(47) Kurtz, R. L.; Stockbauer, R.; Msdey, T. E.; Roman, E.; Desegovia, J. L. *Surf. Sci.* **1989**, *218*, 178.
(48) Zhou, C.; Ma, Z.; Ren, Z.; Wodtke, A. M.; Yang, X. *Energy Environ. Sci.* **2012**, *5*, 6833.
(49) Hugenschmidt, M. B.; Gamble, L.; Campbell, C. T. *Surf. Sci.* **1994**, *302*, 329.
(50) Zhao, J.; Li, B.; Onda, K.; Feng, M.; Petek, H. *Chem. Rev.* **2006**, *106*, 4402.
(51) Henderson, M. A. *Surf. Sci.* **1995**, *343*, L1156.
(52) See, A. K.; Bartynski, R. A. *J. Vac. Sci. Technol., A* **1992**, *10*, 2591.
(53) See, A. K.; Thayer, M.; Bartynski, R. A. *Phys. Rev. B: Condens. Matter Mater. Phys.* **1993**, *47*, 13722.
(54) Glassford, K. M.; Chelikowsky, J. R. *Phys. Rev. B: Condens. Matter Mater. Phys.* **1992**, *46*, 1284.
(55) Labat, F.; Baranek, P.; Domain, C.; Minot, C.; Adamo, C. *J. Chem. Phys.* **2007**, *126*, 154703.
(56) Islam, M. M.; Calatayud, M.; Pacchioni, G. *J. Phys. Chem. C* **2011**, *115*, 6809.

DOI: 10.1021/jacs.5b04483
J. Am. Chem. Soc. 2015, 137, 9146−9152